Synthesis, Characterization, and Photocatalytic Properties of Sol-Gel Ce-TiO_2 Films

Lidija Ćurković *, Debora Briševac, Davor Ljubas *, Vilko Mandić, Ivana Gabelica

Posted Date: 10 May 2024

doi: 10.20944/preprints202405.0652.v1

Keywords: Ce-TiO2; ciprofloxacin; photocatalysis; characterization

Article

Synthesis, Characterization, and Photocatalytic Properties of Sol-Gel Ce-TiO_2 Films

Lidija Ćurković [1,*], Debora Briševac [1], Davor Ljubas [1,*], Vilko Mandić [2] and Ivana Gabelica [1]

[1] Faculty of Mechanical Engineering and Naval Architecture, University of Zagreb, 10000 Zagreb, Croatia; lidija.curkovic@fsb.unizg.hr (L.Ć.); debora.brisevac@fsb.unizg.hr (D.B.); davor.ljubas@fsb.unizg.hr (D.LJ.); ivana.gabelica@fsb.unizg.hr (I.G.)

[2] Faculty of Chemical Engineering and Technology, University of Zagreb, 10000 Zagreb, Croatia; vmandic@fkit.hr (V.M.)

* Correspondence: (L.Ć.); davor.ljubas@fsb.unizg.hr (D.LJ.)

Abstract: In this study, nanostructured cerium-doped TiO_2 (Ce-TiO_2) films with the addition of different amounts of cerium (0.00, 0.08, 0.40, 0.80, 2.40, and 4.10 wt. %) were deposited on a borosilicate glass substrate, by flow coating sol-gel process. After flow coating, deposited films were dried at the temperature of 100 °C for 1 h, followed by calcination at the temperature of 450 °C for 2 h. For the characterization of sol-gel TiO_2 films, the following analytic techniques were used: X-ray diffraction (XRD), thermal gravimetry (TG), differential thermal analysis (DTA), and differential scanning calorimetry (DSC). Sol-gel derived Ce-TiO_2 films were used for photocatalytic degradation of the ciprofloxacin (CIP). The influence of the amount of Ce in TiO_2 films, the duration of the photocatalytic decomposition, and the irradiation type (UV-A and simulated solar light) on the CIP degradation were monitored. Kinetics parameters (reaction kinetics constants and the half-life) of the CIP degradation, as well as photocatalytic degradation efficiency, were determined. The best photocatalytic activity was achieved by the TiO_2 film doped with 0.08 wt.% Ce, under both UV-A, and solar irradiation.

Keywords: Ce-TiO_2; ciprofloxacin; photocatalysis; characterization

1. Introduction

Wastewater released into the environment can have an extremely harmful effect on the nature and well-being of living creatures. Research showed that the most significant amount of pharmaceuticals released into the environment came from wastewater treatment plants [1,2]. The primary sources of pollution are thus sewage collected from households, hospitals, etc. The result of wastewater discharge into the environment is the pollution of soil, surface, underground waters (rivers, lakes, seas) and drinking water [3,4]. In order to reduce or, at best, eliminate pollutants, numerous water and air purification techniques are being developed, such as chemical precipitation, filtration, electrodeposition, adsorption, membrane systems, etc. [5–7]. These conventional water treatment processes are no longer efficient enough for the degradation of complex substances such as pharmaceuticals, their metabolites, or transformation products [1,3]. Advanced oxidation processes (AOPs), especially heterogeneous photocatalysis, have shown their promising ability for degradation through the generation of hydroxyl radicals ($OH^{\bullet}$). These are able to react with the pollutants they come into contact with, serving as powerful oxidizing agents [8,9].

Numerous studies have confirmed that some photocatalysts, such as TiO_2, Fe_2O_3, WO_3, ZnO, CeO_2, CdS, ZnS, MoO_3, ZrO_2, and SnO_2, can be activated by light due to the favorable size of the energy gap, electronic structure with a free conduction band and a filled valence band, and thus break down toxic organic substances in water and air [5,10]. Photocatalysts can completely decompose harmful organic substances into simple compounds such as water, carbon dioxide, and corresponding mineral acids [6,11].

TiO_2 is recognized as an excellent photocatalyst, but due to its relatively high band gap energy of 3.2 eV for the anatase phase and 3.03 eV for the rutile phase, it can only be used when irradiated

 doi:10.20944/preprints202405.0652.v1

with UV radiation λ < 387 nm, which makes up only 3-5% of the total naturally occurring solar radiation [6,8,10–12]. In order to extend the photocatalytic activity of TiO_2 into the visible range of electromagnetic radiation, it is often doped with non-metals (N, S, C, H) [13,14], noble metals (Ag, Au, Pt) [15], transition metals (Ce, Fe) [16], modified with metal semiconductors, co-doped with metals and non-metals, etc. [8,10,16–18].

The sol-gel method for the preparation of nanostructured cerium-doped titania has shown promising results in shifting the photocatalytic activity of TiO_2 into the visible range of irradiation [8,12,19–22]. By increasing the concentration of cerium in TiO_2, the band gap of TiO_2 narrows. Consequently, TiO_2 begins to absorb visible light, shifting its absorption edge from UV to the visible spectrum up to 450 nm. This phenomenon is attributed to potential charge transfer between Ce 4*f* levels. The presence of cerium 4*f* levels is critical in suppressing the recombination of electron-hole pairs, thereby enhancing certain processes. However, excessive doping with cerium may introduce an abundance of recombination centres, thus diminishing the photodegradation capability of the material [8,12,23].

Methods that produce the photocatalyst in powder form are less often used because they require the removal of the photocatalyst from water by filtration and other separation processes, which adds another step during the processing and consumes time and resources. Today, the process of photocatalyst immobilization on various substrates has been increasingly used to avoid the complex removal step [7,24].

The aim of this research is to prepare nanoseized sol-gel cerium doped titania ceramic films (Ce-TiO_2), with the addition of different amounts of Ce, for later use in photocatalytic oxidation experiments. The sol-gel flow coating method was used for the deposition of Ce-TiO_2 films on a borosilicate glass substrate. Ciprofloxacin, one of the most widely used antibiotics in the world, was used as a model pollutant, and its photocatalytic degradation was monitored by UV–Vis measurements.

2. Materials and Methods

2.1. Preparation of Ce-TiO_2 Films

Nanostructured Ce-TiO_2 films were deposited on a borosilicate glass substrate by the sol-gel process using the flow coating method. Borosilicate glass plates with dimensions of 30 × 50 × 2 mm were used as substrates. The substrates were carefully cleaned prior to the process of deposition using the procedure already described in [25].

TiO_2 sols (colloidal solutions) with different amounts of cerium (Ce) were prepared by mixing the following analytical grade reagents: titanium(IV) isopropoxide (TIP, $Ti(OCH(CH_3)_2)_4$, 98%, Sigma–Aldrich, St. Louis, MO, USA) as the precursor, cerium(III) nitrate hexahydrate ($CeN_3O_9{\cdot}6H_2O$, 99.5%, Thermo Fisher Scientific, Waltham, MA, US) as the precursor, i-propyl alcohol (PrOH, C_3H_7OH, 99.9%, Gram-Mol, Zagreb, Croatia) as the solvent, acetylacetone (AcAc. $CH_3(CO)CH_2COCH_3$, 99%+, VWR International, Radnor, PA, USA) as the chelating agent and nitric acid (HN, HNO_3, 65%, Carlo Erba Reagents, Val-de-Reuil, France) as the catalyst. The molar ratio of these reactants in all colloidal solutions was TIP:PrOH:AcAc:HN = 1:35:0.63:0.015 *[26,27]*.

Six sols (colloidal solutions) were prepared:

- TiO_2 sol without the addition of cerium (0.00 wt.% of cerium)
- TiO_2 sol with addition 0.08 wt.% of cerium
- TiO_2 sol with addition 0.40 wt.% of cerium
- TiO_2 sol with addition 0.80 wt.% of cerium
- TiO_2 sol with addition 2.40 wt.% of cerium
- TiO_2 sol with addition 4.10 wt.% of cerium.

Colloidal solutions were stirred vigorously for 2 h, and after that sonicated for 30 min. The prepared sols were deposited on borosilicate glass samples using a flow coating method. The samples were dried at 100 °C for 1 hr and heat-treated at 450 °C for 2 hrs at a heating rate of 3 °C min^{-1}. The deposition process using the flow coating method was repeated three times for each colloidal

 doi:10.20944/preprints202405.0652.v1

solution. The flow chart for the preparation of Ce-TiO_2 films using the sol-gel flow coating method is presented in ***Error! Reference source not found.***.

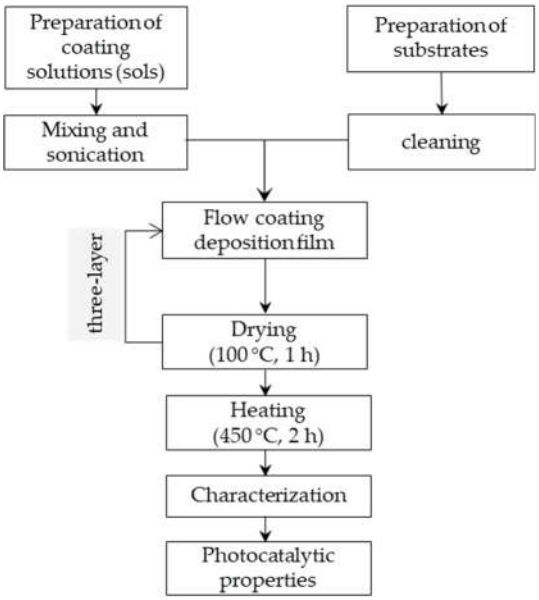

Figure 1. Flow chart for the preparation of Ce-TiO_2 films by sol-gel flow coating method.

2.2. Characterization of Sol-Gel Ce-TiO_2 Films

After the deposition of the sol-gel Ce-TiO_2 films onto a glass substrate, the remaining amounts of colloidal solutions were dried at 60 °C for 24 h in order to produce dried gels. Some amount of the dried gels was used for the analysis by means of thermal gravimetry (TG) and differential scanning calorimetry (DSC). The remaining amount of the dried gels was calcined at a temperature of 450 °C for 2 h and prepared in the form of a powder. These synthesized powders were analyzed in terms of phase compositions as well as parameters and volume of unit cells of Ce-TiO_2 samples by means of X-ray diffraction (XRD) using a D8 Advance Eco diffractometer (Bruker, Billerica, USA) with CuKα radiation (l = 1.54055 A˚) at 40 kV and 25 mA. The thermal characterization of the two samples (TiO_2 without the addition of cerium and TiO_2 with the addition of 0.08 wt.% of cerium was carried out by means of simultaneous differential thermal and thermogravimetric analysis STA 409 (Netzsch , Selb, Germany).

2.3. Adsorption, Photolytic and Photocatalytic Experiments

For experiments (dark adsorption, photolysis, and photocatalysis), analytical grade ciprofloxacin (CIP, 98%, Acros Organics, Waltham, MA, USA) was used as the model organic micropollutant (OMP). Deionized water of ultrapure quality (electrical conductivity of 0.055 μS·cm^{-1} at 25 °C) was used throughout the experiments. The solution of CIP (5 mg·L^{-1}) was prepared by dissolving the appropriate amount of solid in ultrapure quality water. The photocatalytic activity of Ce-TiO_2 films with 0.00, 0.08, 0.40, 0.80, 2.40 and 4.10 wt. % of Ce was evaluated through the degradation of CIP using the following radiation sources: UV-A lamp, model UVAHAND LED (Dr. Hönle AG, UV-Technologie, Gilching, Germany) (peak on 365 nm, 70 W) and solar light simulator (SLS) model SOL500 (Dr. Hönle AG, UV-Technologie, Gilching, Germany (430 W).

The photocatalytic activity of pure TiO_2 and Ce-TiO_2 films with different amounts of cerium was evaluated in a borosilicate glass reactor with a diameter of 95 mm, height of 55 mm, and volume of 250 mL with constant stirring of the investigated solution using a magnetic stirrer at 300 rpm. For the photocatalytic test, in each experiment, 4 glass plates with the photocatalytic film were put on the bottom of the reactor with 100 mL of the CIP solution (5 mg·L^{-1}) as the model OMP and irradiated from above with lamps 20 cm away from the reactor. After that, the lamp was turned on and the suspension was irradiated for 2 hours. Samples were taken from the reactor at intervals (0, 10, 20, 30,

 doi:10.20944/preprints202405.0652.v1

45, 60, 90, 105, and 120 min), filtered using a 0.45 μm mixed cellulose ester membrane filter, and directly analyzed by means of UV-Vis spectrophotometer (HEWLETT PACKARD, Model HP 8430, Palo Alto, CA, USA) at 273 nm (maximum absorption peak of CIP). Before irradiation, the solution was stirred for 15 minutes in the dark to ensure adsorption-desorption equilibrium, determined previously by the adsorption test. Also, the photolytic activity of the CIP solution was tested. Photolytic testing was carried out using the same process, but without adding the prepared photocatalyst films to the reactor.

Pseudo-first-order kinetic models were used to investigate the kinetics of photocatalytic degradation of CIP using the prepared Ce-TiO_2 films. The linear form of the pseudo-first-order kinetic model is described by the following equation [28]:

$$-\ln\frac{A_t}{A_0} = k \cdot t \quad (1)$$

Where k (min^{-1}) is the rate constant of the pseudo-first-order reaction of the photocatalytic decomposition of CIP, A_t is the absorbance of the CIP after irradiation at time, t (min) during the photocatalytic process, and A_0 is the initial absorbance of the CIP.

The half-life ($t_{1/2}$, min) was calculated by the following equation [27]:

$$t_{1/2} = \frac{\ln 2}{k} \quad (2)$$

The photocatalytic degradation efficiency (η, %) of the degradation of CIP by prepared photocatalysts was calculated according to the following equation [29]:

$$\eta = \frac{A_0 - A_t}{A_0} \cdot 100\% \quad (3)$$

where A_0 is the initial absorbance of the CIP, and A_t is the absorbance of the CIP at time t (min) during the photocatalytic process.

3. Results

3.1. Characterization of Photocatalysts

The thermal analysis was carried out in order to determine the mass loss of samples of nanostructured TiO_2 powders and to monitor exothermic and endothermic reactions depending on the temperature. The analysis was carried out on two samples, TiO_2 powder without the addition of Ce and with the addition of 0.08 wt.% Ce. A comparison of DSC/TG curves is shown in **Error! Reference source not found.**. Changes were observed in the temperature interval from room temperature to 1000 °C. During the heating of both samples, there was an increase in their mass loss, which is characteristic for the thermal decomposition of amorphous gels.

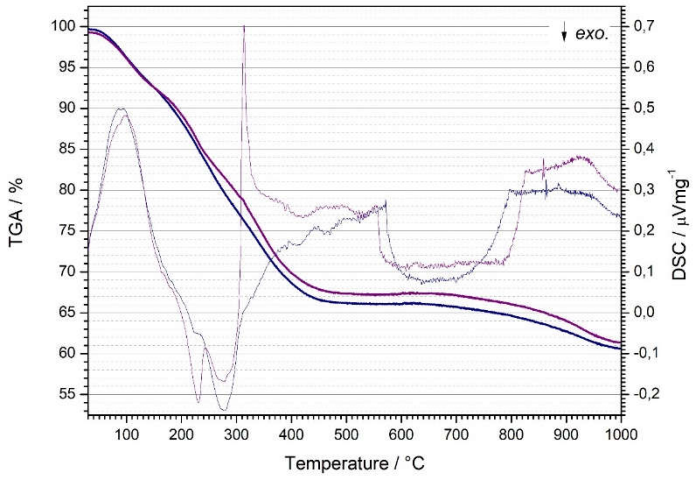

 doi:10.20944/preprints202405.0652.v1

Figure 2. DSC/TG curves for TiO_2 without addition Ce (purple line) and TiO_2 with addition of 0.08 wt.% Ce (blue line).

Two mass losses can be observed from the curves for both samples. In the area of lower temperatures, mass loss occurs due to the release of solvent and chemisorbed water, while around medium temperatures, decomposition and combustion of hydroxyl groups ($OH^{\bullet}$) and organic phases present in the samples occur. The total mass loss of the TiO_2 sample without the addition of Ce is slightly higher than the mass loss of the TiO_2 sample with the addition of 0.08 wt.% Ce. When samples are heated, processes occur that are accompanied by the release (exothermic reactions) or the receipt of heat (endothermic reactions), i.e., a decrease or increase in the temperature of the samples in relation to the reference material, which is recorded as minima and maxima on the DSC curves. Both samples (TiO_2 and 0.08 wt. % Ce-TiO_2) have an endothermic minimum and exothermic maximum. The endothermic minimum is attributed to the desorption and release of substances from the gel, such as adsorbed water and alcohol. The exothermic maximums are attributed to the desorption of hydroxyl groups and other organic phases and the crystallization of the anatase phase of titanium dioxide. In the case of the 0.08 wt.% Ce-TiO_2 sample, a more complex course of thermal evolution with more pronounced multi-stage effects is visible, which is in accordance with the more complex composition of the precursor. In the case of the doped sample (0.08 wt.% Ce-TiO_2), anatase crystallization is shifted towards higher temperatures. In conclusion, the samples basically do not differ in the early stage of solvent loss, but undoped samples went through more abrupt multistage exothermic events around 300°C. The composition probably allowed more significant auto-combustion behaviour during heating. Importantly, above 450°C the mass loss remains fairly constant (slightly less for the undoped sample), meaning the volatiles were removed. Only above 800°C the carbon remains are burned off resulting is additional slight mass loss.

XRD results point to crystallization of TiO_2 predominatelly in anatase structure, however thtaces of rutile structure have been observed (**Error! Reference source not found.**). Results of the XRD analysis of TiO_2 samples with different amounts (wt.%) of Ce (0.00, 0.08, 0.40, 0.80, 2.40, and 4.10) are presented in **Error! Reference source not found.**. Obtained results showed that 0.08 wt.%, Ce is easily incorporated into the TiO_2 lattice. **Error! Reference source not found.**With further increase of Ce amount, the rutile phase is absent, and Ce incorporation into the TiO_2 lattice significantly reduces. The crystallite size decreases linearly with increasing Ce content from 45.8 nm (pure TiO_2) to 11.2 nm (TiO_2 with 4.1 wt.% of Ce). In the samples with 2.40 wt.% Ce-TiO_2 and 4.10 wt.% Ce-TiO_2, there are barely any traces of the cerium oxide phase.

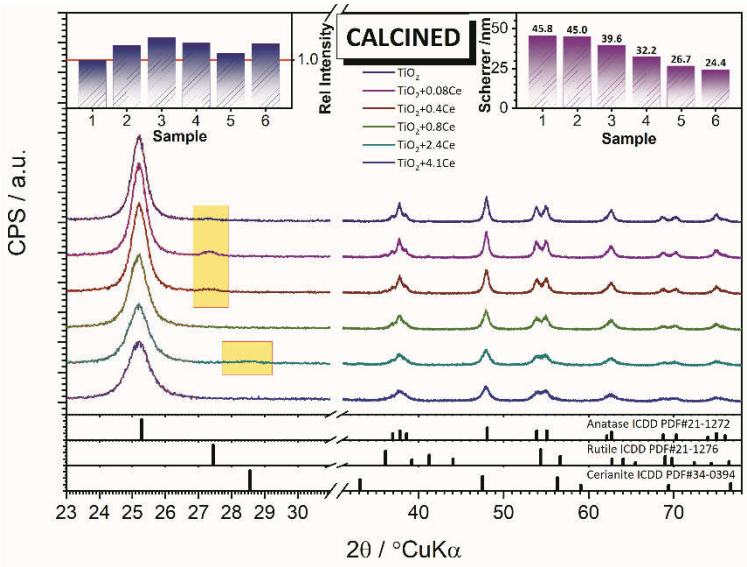

Figure 3. X-ray diffraction patterns and crystallite size TiO_2 samples with different amounts (wt. %) of Ce: 0.00, 0.08, 0.40, 0.80, 2.40, and 4.10.

Preprints.org (www.preprints.org) | NOT PEER-REVIEWED | Posted: 10 May 2024 doi:10.20944/preprints202405.0652.v1

The amount of incorporated Ce in the TiO_2 unit cell depends on the difference in the crystal radius of Ce^{4+} and Ti^{4+}. From the values of the parameters and the volume of the unit cell (**Error! Reference source not found.**), it can be seen that smaller amounts of cerium (up to 0.08 wt.%) can be easily incorporated into the unit cell of anatase while doping with Ce in amounts greater than 0.08 wt. % again leads to a decrease in parameter values and volume, which is a consequence of the difficulty of incorporating Ce^{4+} ions into the anatase unit cell. The radius of Ce^{4+} ions (0.092 nm) is much larger than the radius of Ti^{4+} ions (0.065 nm), so it is to be expected that a minimal amount of Ce^{4+} can be incorporated into the TiO_2 lattice and that an increase in the amount of Ce will result in the crystallization of additional separated phases of cerium oxide [24]. This behavior of the system is in accordance with the qualitative diffraction analysis.

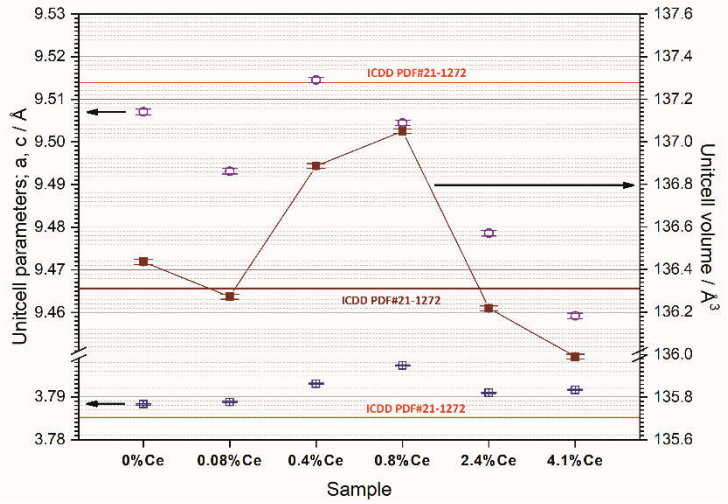

Figure 4. Parameters and volume of unit cells of TiO_2 samples with different amounts (wt. %) of Ce: 0.00, 0.08, 0.40, 0.80, 2.40, and 4.10.

3.2. Photocatalytic Properties of TiO_2 and Ce-TiO_2 Films

The photoactivity of the TiO_2 films with the different amounts (wt.%) Ce (0.00, 0.08, 0.40, 0.80, 2.40, and 4.10) was evaluated through the degradation of CIP aqueous solution (5 mg·L^{-1}) under the UVA light (***Error! Reference source not found.***A) and solar light simulator (***Error! Reference source not found.***B). ***Error! Reference source not found.*** shows the kinetics of photolytic and photocatalytic degradation of CIP, i.e., the dependence of the change in the relative absorbance value (A/A_0) versus time (t, min). Before the photocatalytic test, dark adsorption (D. A.) was performed (***Error! Reference source not found.***A and 5B). The initial pH of the CIP solution was in the range of 6.3 – 6.5; after the experiments (adsorption, photolysis, and photocatalysis), the pH values were kept the same. Dark adsorption of ciprofloxacin on TiO_2 and Ce-TiO_2 films was negligible. The best photocatalytic properties were achieved by TiO_2 film doped with 0.08 wt. % of Ce by UV-A (365 nm) and solar light simulator radiation. For all Ce-TO_2 films, better photocatalytic properties were achieved by solar light simulator radiation compared to UV-A (365 nm) radiation.

Preprints.org (www.preprints.org) | NOT PEER-REVIEWED | Posted: 10 May 2024 doi:10.20944/preprints202405.0652.v1

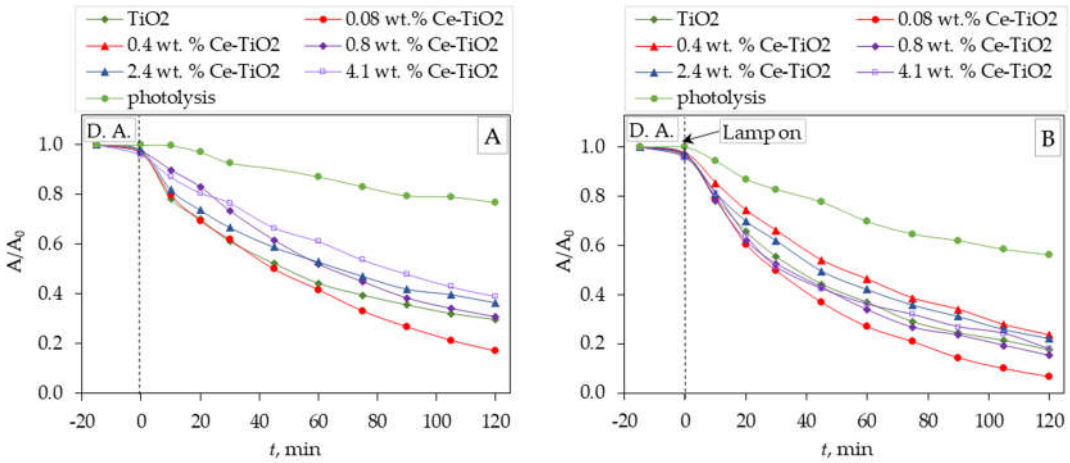

Figure 5. Photolytic and photocatalytic degradation of CIP under (**A**) UV-A (365 nm) and (**B**) solar light simulator radiation by sol-gel Ce-TiO_2 films as a function of irradiation time, γ_0 (CIP) = 5 mg·L^{-1}.

The photolytic and photocatalytic data are described using the pseudo-first-order model. The pseudo-first-order rate constant k from Eq. (1) is evaluated through the linear regression of -ln (A/A_0) versus t (***Error! Reference source not found.***). The pseudo-first-order model describes a process in which the degradation rate is mainly affected by changes in pollutant concentration [30].

The kinetic constant for the pseudo-first-order is obtained from the slope of the plot of -ln (A/A_0) versus the irradiation time (***Error! Reference source not found.***).

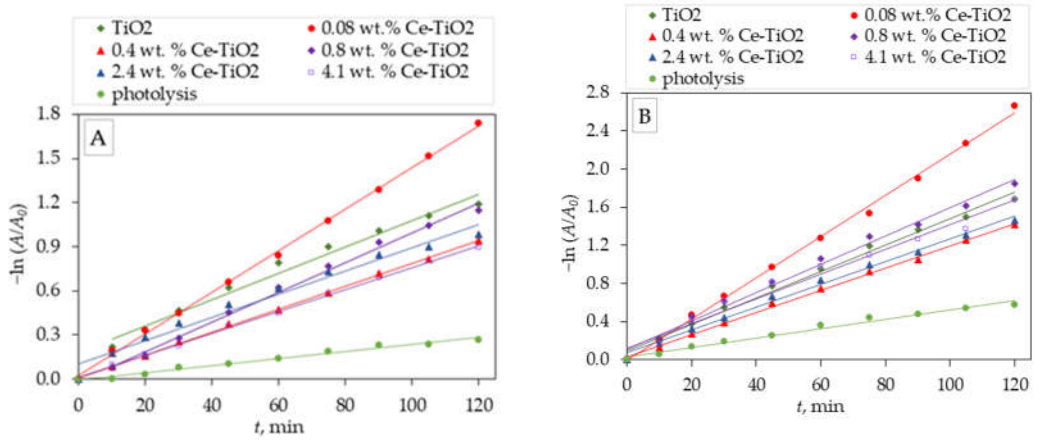

Figure 6. Linear transform of −ln (A/A_0) versus t of photolytic and photocatalytic degradation of CIP under (**A**) UV-A (365 nm) and (**B**) solar light simulator radiation by sol-gel Ce-TiO_2 films, γ_0 (CIP) = 5 mg·L^{-1}.

Calculated values of the pseudo-first-order (k, min^{-1}), the half-life ($t_{1/2}$, min), and the removal efficiencies of Ce-TiO_2 films are listed in ***Error! Reference source not found.***. The pseudo-first-order model shows that under the UV and solar light, the correlation coefficient (R^2) in all cases has a value above 0.98, indicating that the pseudo-first model describes both experimental degradation processes (photocatalytic and photolytic) well. A comparisons of the obtained values of pseudo-first-order (k, min^{-1}) and removal efficiencies (η, %) for all experimental conditions are presented in ***Error! Reference source not found.***A and 7B, respectively. From the photocatalytic tests, it can be seen that the TiO_2 film with the least addition of Ce (0.08 wt.%) has the highest photocatalytic efficiency and the highest CIP degradation rate constant for both radiation sources (***Error! Reference source not found.*** and ***Error! Reference source not found.***). By comparing the photocatalytic activity of the same films with both radiation sources, it can be observed that a higher photocatalytic efficiency and a higher degradation rate constant were achieved by applying solar light simulator radiation.

 doi:10.20944/preprints202405.0652.v1

 doi:10.20944/preprints202405.0652.v1

Table 1. The values of pseudo-first-order reaction rate constants (k, min^{-1}) and half-life times ($t_{1/2}$, min), along with the corresponding correlation coefficients (R^2) and removal efficiency of photocatalytic degradation of ciprofloxacin (γ_0 = 5 mg L^{-1}) by TiO_2 films with different amounts of Ce, under UV-A and SOLAR radiation, at a temperature of 25 °C.

Film	UV-A				Solar light simulator			
	$k \times 10^{-3}$, min^{-1}	$t_{1/2}$, min	R^2	h, %	$k \times 10^{-3}$, min^{-1}	$t_{1/2}$, min	R^2	h, %
Photolysis (without film)	2.4	288.81	0.9840	23.35	4.9	141.46	0.9835	43.88
0 wt.% Ce-TiO_2	8.9	77.88	0.9815	67.53	13.9	49.87	0.9907	81.54
0.08 wt.% Ce-TiO_2	**14.1**	49.16	0.9989	**82.38**	**21.6**	32.09	0.9977	**93.04**
0.40 wt.% Ce-TiO_2	7.8	88.87	0.9991	61.03	11.7	59.24	0.9980	75.79
0.80 wt.% Ce-TiO_2	10.0	68.63	0.9945	68.22	14.6	47.48	0.9934	84.28
2.40 wt.% Ce-TiO_2	7.6	91.20	0.9863	62.58	12.0	57.76	0.9938	76.92
4.10 wt.% Ce-TiO_2	7.4	93.67	0.9990	59.12	12.7	54.58	0.9810	81.32

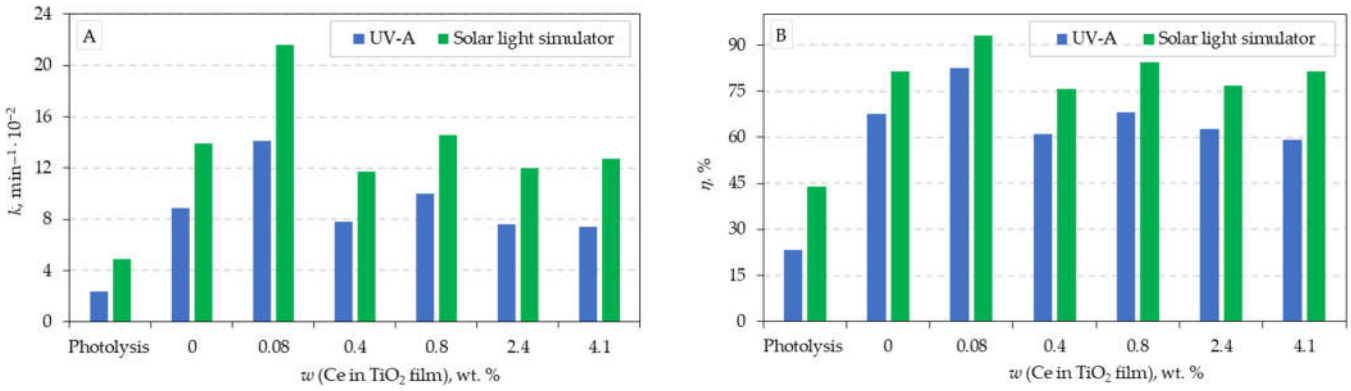

Figure 7. Comparison of the values of (**A**) pseudo-first-order kinetic constants and (**B**) degradation efficiency of photolytic and photocatalytic degradation of CIP under UV-A (365 nm) and solar light simulator radiation by sol-gel Ce-TiO_2 films, γ_0 (CIP) = 5 mg·L^{-1}.

Martins et al. prepared Au/TiO_2 nanocomposite (Au loading ranging from 0.025 to 0.5 wt.%) for photocatalytic degradation of CIP (5mg·L^{-1}) under UV and simulated visible light. Reaction rate constants varied from 0.047 to 0.131 min^{-1} for different Au loading over 30 minutes of UV irradiation, while apparent reaction rates over 180 minutes of visible light irradiation varied from 0.073 to 0.242 min^{-1} for different Au loading [31].

To overcome the separation process of photocatalyst, Hassani et al. employed the immobilization of TiO_2 onto montmorillonite for the degradation of 20 mg·L^{-1} ciprofloxacin. In contrast to suspended TiO_2, which degraded only 57% (with a rate constant of 0.0063 min^{-1}), the immobilized TiO_2 exhibited accelerated degradation (0.0069 min^{-1}) and achieved up to 62% degradation within 2 hours [32].

 doi:10.20944/preprints202405.0652.v1

Malakootian et al. also immobilized TiO_2 nanoparticles on a glass plate for photocatalytic degradation of CIP (5mg·L^{-1}) under UV light. The reaction rate constant was 0.0193 min^{-1}, and removal efficiency was around 60% after 60 minutes of irradiation [33].

Different light sources as well as metal and non-metal doping of TiO_2 were widely investigated by numerous scientists for the degradation of ciprofloxacin. Their results are summarized by Imam et al. [34].

4. Conclusions

This paper presents the results of the photolytic and photodegradation process of a diazo CIP aqueous solution in the presence of Ce-TiO_2 films under UV-A (365 nm) and solar light simulator radiation. Six sol-gel TiO_2 films with different amounts of Ce (0.00, 0.08, 0.40, 0.80, 2.40, and 4.10 wt.%) were deposited on a glass substrate by a flow coating method.

The crystallite size, as well as phase composition are changed by changing the amount of Ce in TiO_2 samples.

These results indicate that the photocatalytic properties of sol-gel TiO_2 films depend on the amount of added Ce.

The mechanisms of photocatalytic oxidation of the CIP by sol-gel TiO_2 films were described by a pseudo-first-order kinetic model. The obtained values of the determination coefficient R^2 (all values were above 0.98) indicate that the pseudo-first-order rate is suitable for describing the photodegradation process of CIP photocatalytic degradation with sol-gel Ce-TiO_2 films as the photocatalyst.

It was found that sol-gel TiO_2 film with the least addition of Ce (0.08 wt.%) has the highest photocatalytic efficiency and the highest CIP degradation rate constant for both radiation sources. Comparing the photocatalytic activity of the same films with both radiation sources, it can be concluded that applying solar light simulator radiation achieved a higher photocatalytic efficiency and a higher degradation rate constant. This could be used for further use of natural solar radiation in real wastewater treatment plants for degradation of OMPs.

Author Contributions: Conceptualization, L.Ć., D.Lj. and D.B.; methodology, L.Ć., D.Lj. and D.B.; software, L.Ć., D.Lj., V.M., D.B. and I.G.; validation, , L.Ć., D.Lj., V.M., D.B. and I.G.; formal analysis, D.B., V.M. and I.G.; investigation, D.B.; resources, L.Ć., D.Lj. and V.M.; data curation, L.Ć., D.Lj., V.M., D.B. and I.G.; writing—original draft preparation, L.Ć., D.B., D.Lj. and I.G.; writing—review and editing, , L.Ć., D.Lj., V.M., D.B. and I.G.; visualization, , L.Ć., D.Lj., V.M., D.B. and I.G.; supervision, D.Lj. and L.Ć.; project administration, L.Ć., and D.Lj.; funding acquisition, L.Ć., and D.Lj. All authors have read and agreed to the published version of the manuscript.

Funding: This work was funded by the Croatian Science Foundation under the project [IP-2016-06-6000]: Monolithic and Composite Advanced Ceramics for Wear and Corrosion Protection (WECOR).

Data Availability Statement: The data presented in this study are available upon reasonable request from the corresponding author.

Conflicts of Interest: The authors declare no conflict of interest.

References

1. Čizmić, M.; Ljubas, D.; Rožman, M.; Ašperger, D.; Ćurković, L., Babić, S. Photocatalytic Degradation of Azithromycin by Nanostructured TiO_2 Film: Kinetics, Degradation Products, and Toxicity. *Materials* **2019**, *12*, 873.
2. Ljubas, D.; Čizmić, M.; Vrbat, K.; Stipaničev, D.; Repec, S.; Ćurković, L.; et al. Albendazole Degradation Possibilities by UV-Based Advanced Oxidation Processes. *Int. J. Photoenergy*. **2018**, *6*, 6181747.
3. Santos, L.H.M.L.M.; Araújo, A.N.; Fachini, A.; Pena, A.; Delerue-Matos, C.; Montenegro, M.C.B.S.M. Ecotoxicological aspects related to the presence of pharmaceuticals in the aquatic environment. *J. Hazard. Mater.* **2010**, *175*, 45-95.
4. Babić, S.; Zrnčić, M.; Ljubas, D.; Ćurković, L.; Škorić, I. Photolytic and thin TiO_2 film assisted photocatalytic degradation of sulfamethazine in aqueous solution. *Environ. Sci. Pollut. Res.* **2015**, *22*, 11372-86.
5. Etacheri, V.; Di Valentin, C.; Schneider, J.; Bahnemann, D.; Pillai, S.C. Visible-light activation of TiO_2 photocatalysts: Advances in theory and experiments. *J. Photoch. Photobio. C* **2015**, *25*, 1-29.

6. Teh, C.M.; Mohamed, A.R. Roles of titanium dioxide and ion-doped titanium dioxide on photocatalytic degradation of organic pollutants (phenolic compounds and dyes) in aqueous solutions: A review. *J. Alloy. Compd.* **2011**, *509*, 1648-60.
7. Čizmić, M.; Ljubas, D.; Ćurković, L.; Škorić, I.; Babić, S. Kinetics and degradation pathways of photolytic and photocatalytic oxidation of the anthelmintic drug praziquantel. *J. Hazard. Mater.* **2017**, *323*, 500-12.
8. Cerrato, E.; Gaggero, E.; Calza, P.; Paganini, M.C. The role of Cerium, Europium and Erbium doped TiO_2 photocatalysts in water treatment: A mini-review. *Chem. Eng. J.* **2022**, *10*, 100268.
9. Shan, A.Y.; Ghazi, T.I.M.; Rashid, S.A. Immobilisation of titanium dioxide onto supporting materials in heterogeneous photocatalysis: A review. *Appl. Catal. A-Gen.* **2010**, *389*, 1-8.
10. Umar, K.; Aris, A.; Ahmad, H.; Parveen, T.; Jaafar, J.; Majid, Z.A.; et al. Synthesis of visible light active doped TiO_2 for the degradation of organic pollutants—methylene blue and glyphosate. *J. Anal. Sci. Technol.* **2016**, *7*, 29.
11. Lan, Y.; Lu, Y.; Ren, Z. Mini review on photocatalysis of titanium dioxide nanoparticles and their solar applications. *Nano Energy*. **2013**, *2*, 1031-45.
12. Marami, M.B.; Farahmandjou, M. Water-Based Sol–Gel Synthesis of Ce-Doped TiO_2 Nanoparticles. *J. Electron. Mater.* **2019**, *48*, 4740-7.
13. Li, G.; Zou, B.; Feng, S.; Shi, H.; Liao, K.; Wang, Y.; et al. Synthesis of N-Doped TiO_2 with good photocatalytic property. *Phys. B: Condens. Matter*. **2020**, *588*, 412184.
14. Yan, J.; Zhao, J.; Hao, L.; Hu, Y.; Liu, T.; Guan, S.; et al. Low-temperature S-doping on N-doped TiO_2 films and remarkable enhancement on visible-light performance. *Mater. Res. Bull.* **2019**, *120*, 110594.
15. Mahmoudian-Boroujerd, L.; Karimi-Jashni, A.; Hosseini, S.N.; Paryan, M. Optimization of rDNA degradation in recombinant Hepatitis B vaccine production plant wastewater using visible light excited Ag-doped TiO_2 nanophotocatalyst. *Process Saf. Environ. Prot.* **2019**, *122*, 328-38.
16. Kayani, Z.N.; Maria; Riaz, S.; Naseem, S. Magnetic and antibacterial studies of sol-gel dip coated Ce doped TiO_2 thin films: Influence of Ce contents. *Ceram. Int.* **2020**, *46*, 381-90.
17. Contreras-García, M.E.; García-Benjume, M.L.; Macías-Andrés, V.I.; Barajas-Ledesma, E.; Medina-Flores, A.; Espitia-Cabrera M.I. Synergic effect of the TiO_2-CeO_2 nanoconjugate system on the band-gap for visible light photocatalysis. *Mater. Sci. Eng.: B.* **2014**, *183*, 78-85.
18. Abdullah, H.; Khan, M.R.; Pudukudy, M.; Yaakob, Z.; Ismail, N.A. CeO_2-TiO_2 as a visible light active catalyst for the photoreduction of CO_2 to methanol. *J. Rare Earths.* **2015**, *33*, 1155-61.
19. Sun, P.; Liu, L.; Cui, S.C., Liu, J.G. Synthesis, Characterization of Ce-doped TiO_2 Nanotubes with High Visible Light Photocatalytic Activity. *Catal. Lett.* **2014**, *144*, 2107-13.
20. Choudhury, B.; Borah, B.; Choudhury, A. Extending Photocatalytic Activity of TiO_2 Nanoparticles to Visible Region of Illumination by Doping of Cerium. *Photochem. Photobiol.* **2012**, *88*, 257-64.
21. Chen, F.; Ho, P.; Ran, R.; Chen, W.; Si, Z.; Wu, X.; et al. Synergistic effect of CeO_2 modified TiO_2 photocatalyst on the enhancement of visible light photocatalytic performance. *J. Alloy. Compd.* **2017**, *714*, 560-6.
22. Shaari, N.; Tan, S.H.; Mohamed, A.R. Synthesis and characterization of CNT/Ce-TiO_2 nanocomposite for phenol degradation. *J. Rare Earths* **2012**, *30*, 651-8.
23. Lee, J.Y.; Choi, J.H. Sonochemical Synthesis of Ce-doped TiO_2 Nanostructure: A Visible-Light-Driven Photocatalyst for Degradation of Toluene and O-Xylene. *Materials* **2019**, *12*, 1265.
24. Cao, X.P.; Li, D.; Jing, W.H.; Xing, W.H.; Fan, Y.Q. Synthesis of visible-light responsive C, N and Ce co-doped TiO_2 mesoporous membranes via weak alkaline sol–gel process. *J. Mater. Chem.* **2012**, *22*, 15309-15.
25. Šegota, S.; Ćurković, L.; Ljubas, D.; Svetlicic, V.; Houra, I.; Tomasic, N. Synthesis, characterization and photocatalytic properties of Sol-gel TiO_2 films. *Ceram. Int*. **2011**, *37*, 1153-60.
26. Ćurković, L.; Ljubas, D.; Šegota, S.; Bačić, I. Photocatalytic degradation of Lissamine Green B dye by using nanostructured sol–gel TiO_2 films. *J. Alloy. Compd.* **2014**, *604*, 309-16.
27. Švagelj, Z.; Mandić, V.; Ćurković, L.; Biošić, M.; Žmak, I.; Gaborardi, M. Titania-Coated Alumina Foam Photocatalyst for Memantine Degradation Derived by Replica Method and Sol-Gel Reaction. *Materials* **2020**, *13*, 227.
28. Sanchez Tobon, C.; Ljubas, D.; Mandić, V.; Panžić, I.; Matijašić, G.; Ćurković, L. Microwave-Assisted Synthesis of N/TiO_2 Nanoparticles for Photocatalysis under Different Irradiation Spectra. *Nanomaterials* **2022**, *12*, 1473.
29. Gabelica, I.; Ćurković, L.; Mandić, V.; Panžić, I.; Ljubas, D.; Zadro, K. Rapid Microwave-Assisted Synthesis of Fe_3O_4/SiO_2/TiO_2 Core-2-Layer-Shell Nanocomposite for Photocatalytic Degradation of Ciprofloxacin. *Catalysts* **2021**, *11*, 1136.
30. Ngo, H.S.; Nguyen, T.L.; Tran, N.T.; Le, H.C. Experimental Study on Kinetics and Mechanism of Ciprofloxacin Degradation in Aqueous Phase Using Ag-TiO_2/rGO/Halloysite Photocatalyst. *Catalysts* **2023**, *13*, 225.
31. Martins, P.; Kappert, S.; Nga Le, H.; Sebastian, V.; Kühn, K.; Alves, M.; et al. Enhanced Photocatalytic Activity of Au/TiO_2 Nanoparticles against Ciprofloxacin. *Catalysts* **2020**, *10*, 234.

 doi:10.20944/preprints202405.0652.v1

32. Hassani, A.; Khataee, A.; Karaca, S.; Fathinia, M. Heterogeneous photocatalytic ozonation of ciprofloxacin using synthesized titanium dioxide nanoparticles on a montmorillonite support: parametric studies, mechanistic analysis and intermediates identification. *RSC Adv.* **2016**, *6*, 87569-83.
33. Malakootian, M.; Nasiri, A.; Amiri Gharaghani, M. Photocatalytic degradation of ciprofloxacin antibiotic by TiO_2 nanoparticles immobilized on a glass plate. *Chem. Eng. Commun.* **2020**, *207*, 56-72.
34. Shehu Imam, S.; Adnan, R.; Mohd Kaus, N.H. Photocatalytic degradation of ciprofloxacin in aqueous media: a short review. *Toxicol. Environ. Chem.* **2018**, *100*, 518-39.